



## Article

# Identification and Expression Analysis of the *bHLH* Gene Family Members in *Diospyros kaki*

Weijuan Han <sup>1</sup>, Qi Zhang <sup>1,2</sup> , Yujing Suo <sup>1</sup>, Huawei Li <sup>1</sup>, Songfeng Diao <sup>1</sup>, Peng Sun <sup>1</sup> , Lin Huang <sup>1,\*</sup> and Jianmin Fu <sup>1,\*</sup>

<sup>1</sup> Research Institute of Non-Timber Forestry, Chinese Academy of Forestry, Key Laboratory of Non-Timber Forest Germplasm Enhancement & Utilization of State Administration of Forestry and Grassland, No. 3 Weiwu Road, Jinshui District, Zhengzhou 450003, China

<sup>2</sup> College of Forestry, Inner Mongolia Agricultural University, Hohhot 010018, China

\* Correspondence: huanglinzz@163.com (L.H.); fjm371@163.com (J.F.)

**Abstract:** Basic helix–loop–helix (bHLH) proteins belong to one of the largest families involved in plant growth, development, signal transduction, and secondary metabolism. Although *bHLH* genes have been previously identified in persimmon (*Diospyros kaki*), systematic studies have not been reported. A total of 59 *bHLH* family members have been identified from the “Xiaoguotianshi” persimmon transcriptome. These proteins were clustered into 12 groups from I to XII based on their phylogenetic relationships with *Arabidopsis thaliana*. Combined with the phylogenetic analysis, in silico expression patterns of five developmental stages, the protein–protein interaction analysis between DkbHLH and DkMYB proteins showed that the bHLH\_Cluster-15548.1 protein sequence was identified to be highly similar to the AtGL3 (AT5G41315.1) protein, which is associated with flavonoid and proanthocyanidin (PA) biosynthesis. This study presents the systematic analysis of *bHLH* genes from *D. kaki* and provides valuable information for further research on the involvement of bHLH protein in anthocyanin biosynthesis.

**Keywords:** proanthocyanidin (PA) biosynthesis; gene family; *bHLH* genes; persimmon; bioinformatics



**Citation:** Han, W.; Zhang, Q.; Suo, Y.; Li, H.; Diao, S.; Sun, P.; Huang, L.; Fu, J. Identification and Expression Analysis of the *bHLH* Gene Family Members in *Diospyros kaki*.

*Horticulturae* **2023**, *9*, 380. <https://doi.org/10.3390/horticulturae9030380>

Academic Editors: Dario Paolo, Chiara Mizzotti and Francesco Vuolo

Received: 11 February 2023

Revised: 12 March 2023

Accepted: 13 March 2023

Published: 15 March 2023



**Copyright:** © 2023 by the authors. Licensee MDPI, Basel, Switzerland. This article is an open access article distributed under the terms and conditions of the Creative Commons Attribution (CC BY) license (<https://creativecommons.org/licenses/by/4.0/>).

## 1. Introduction

Persimmon (*Diospyros kaki*) is an important fruit tree. The high soluble proanthocyanin content leads to the astringency taste of persimmon fruits, the key characteristic of persimmon. Transcription factors (TFs) involved in proanthocyanin biosynthesis have been identified previously; for example, the R2R3MYB, bHLH, and WD40 (MBW) complex regulates the structural genes of the flavonoid/phenylpropanoid pathway. Basic helix–loop–helix (bHLH) proteins belong to one of the largest families involved in plant growth, development, signal transduction, and secondary metabolism [1–3]. bHLH proteins contain two conserved domains: (1) the HLH domain consisting of two functional segments (the basic and helix–loop–helix (HLH) regions), which possesses approximately 50–60 amino acids, and (2) the bHLH-MYC\_N domain consisting of approximately 15–17 amino acids. The *bHLH* gene family has been recently identified in different plants including *Arabidopsis* [4], potato [5], tomato [6], apple [7], and rice [8]. Furthermore, 162 *Arabidopsis* AtbHLH proteins phylogenetically cluster into 26 subfamilies [4].

The *bHLH* family members, particularly the *bHLH* III (d and e) subfamily genes, play important roles in regulating anthocyanin biosynthesis via the jasmonic acid signaling pathway. In addition, the III (f) subfamily is involved in anthocyanin synthesis [9,10]. The first anthocyanin accumulation-regulating *bHLH* genes R and B were identified and characterised in maize [11]. The *GLABRA3* (*AtbHLH1*) gene in group III (f), encoding an R homolog, is essential for anthocyanin biosynthesis and trichome formation in *A. thaliana* [12]. Overexpression of the III (f) subfamily member VdbHLH037 in grapes increases the accumulation of anthocyanins [13].

Multiple studies have indicated that *bHLH* gene family members regulate anthocyanin and proanthocyanin biosynthesis via interaction with MYB members [14]. For example, *bHLH* members (i.e., R1 and B1) are involved in purple anthocyanin synthesis by interacting with R2R3-MYB members C1 and PL1 [15,16]. *MYB10.1* and *MYB10.3* interact with *bHLH3* to activate anthocyanin production in peaches by regulating *NtCHS*, *NtDFR*, and *NtUGT* [17]. *VvMYC1* interacts with MYB family members to mediate the PA biosynthesis in grapes by inducing gene promoters in the flavonoid pathway [18]. The overexpression of *Arabidopsis CPC* and *GL3* in tomatoes enhances anthocyanin accumulation [19].

This study identified 59 *bHLH* transcription factors from the *D. kaki* transcriptome data. Their phylogenetic relationships, motifs, and expression patterns at different developmental stages were analysed to identify the *bHLH* gene family members that may be associated with PA biosynthesis. This study provides a basic understanding of the *bHLH* gene association with natural astringency loss in Chinese pollination-constant non-astringent (C-PCNA) persimmon.

## 2. Materials and Methods

### 2.1. Plant Materials

*Diospyros kaki* Thunb. ‘Xiaoguotianshi’ cultivar plants were grown in Yuanyang County, Henan Province, China (34°55′18″~34°56′27″ N, 113°46′14″~113°47′35″ E). Five different stages (T1 = 70, T2 = 100, T3 = 120, T4 = 140, T5 = 160 days after flowering (DAF)) of persimmon fruit flesh were flash frozen in liquid nitrogen and stored at −80 °C for further analysis.

### 2.2. RNA Sequencing

‘Xiaoguotianshi’ transcriptome data were collected from a previously published study [20]. A total of 15 cDNA libraries (three independent biological replicates) of fruit samples (T1–T5) were constructed for RNA-Seq. Transcriptome sequencing was performed by the Beijing Novogene Bioinformatics Technology Company (Beijing, China).

### 2.3. Identification of *bHLH* Transcription Factors (TFs) in the *D. kaki* Transcriptome

All putative *bHLH* sequences were queried from the previously published *D. kaki* transcriptome using “*bHLH*”. Pfam rechecked and filtered the predicted sequences (<https://pfam.xfam.org/> (accessed on 12 June 2022)) [21] and the NCBI-CDD online software. The molecular weight (MW), isoelectric point (pI), and instability index of the proteins were calculated using the ExPASy server (<https://www.expasy.org/> (accessed on 14 June 2022)) [22].

### 2.4. Multiple Sequence Alignment, Conserved Motif Identification, and Phylogenetic Analysis

To investigate the phylogenetic relationship of the *bHLH* gene families between *D. kaki* and *A. thaliana*, *AtbHLH* proteins were downloaded from the Plant Transcription Factor Database (<http://planttfdb.gao-lab.org/index.php> (accessed on 18 June 2022)), with redundant sequences removed [23–25]. *bHLH* proteins were aligned using the ClustalX 2 program [26]. A phylogenetic tree was constructed for these proteins using the neighbour-joining (NJ) method with 1,000 bootstrap reiterations using MEGA5.0 software [27]. *DkbHLH* proteins were classified according to the distance between the homologous sequences of *A. thaliana* [28]. MEME v5.0.0 online software (<https://meme-suite.org/tools/meme> (accessed on 22 June 2022)) was used to identify motifs with default parameters, with the maximum number of motifs set to nine [29].

### 2.5. Gene Ontology Annotation

Gene Ontology (GO) enrichment analysis of the identified *DkbHLH* proteins was analysed and visualised using agriGO (<http://bioinfo.cau.edu.cn/agriGO/index.php> (accessed on 2 July 2022)). The results of the GO analysis were grouped into three categories: biological process, cellular component, and molecular function.

## 2.6. Protein Interaction Network Analysis

All putative bHLH sequences were queried from the previously published *D. kaki* transcriptome using “MYB”. The interaction network between DkbHLH and DkMYB proteins using *A. thaliana* on the String protein interaction database (<http://string-db.org/> (accessed on 14 July 2022)) [30].

## 2.7. Calculating Ka and Ks of the Homologous bHLH Gene Pairs

Non-synonymous substitutions per non-synonymous site (Ka) and synonymous substitutions per synonymous site (Ks) were used to assess the selection pressure and divergence time of the bHLH gene family [31]. The number of Ks and Ka of the orthologous bHLH gene pairs between *A. thaliana* and *D. kaki* and the paralogous DkbHLH gene pairs were calculated using the TBtools v1.0971 software [32]. The divergence time (T) of the duplication events was calculated using the formula  $T = Ks / (2 \times 6.1 \times 10^{-9}) \times 10^{-6}$  million years ago (MYA) [33].

## 2.8. In Silico Analysis of bHLH Genes in Different Tissues

To analyse the expression levels of DkbHLH genes during fruit development, the expression profiles of these genes at five different fruit developmental stages were represented using the Fragments Per Kilobase per Million (FPKM) value of the high-throughput sequencing data. The heatmap was generated using the log10-transformed FPKM values. The expression heatmaps and k-means clustering of DkbHLH genes were performed and generated using HEATMAP tools in Hiplot (<https://hiplot.com.cn> (accessed on 28 July 2022)) [34].

## 3. Results

### 3.1. Identification and Phylogenetic Analysis of bHLH Genes in *A. thaliana* and *D. kaki*

Following the removal of the redundant sequences without complete conserved domains, a total of 59 DkbHLH proteins were identified from the *D. kaki* transcriptome. The molecular weights of these DkbHLH proteins ranged from 8641.81 (Cluster-6987.43499) to 79,061.33 Da (Cluster-6987.28853), and the theoretical isoelectric points (pI) ranged from 4.52 (Cluster-6987.10953) to 10.79 (Cluster-17857.0). The length of these proteins varied from 76 (Cluster-6987.43499) to 720 amino acids (Cluster-6987.28853) with an average length of 334 aa (Table 1). The instability index ranged from 34.57 (Cluster-6987.29876) to 93.67 (Cluster-6987.40617), and only two DkbHLH proteins (Cluster-6987.29876 and Cluster-6987.44311) were stable in vitro. The DkbHLH protein GRAVY values ranged from −0.016 (Cluster-6987.29876) to −0.841 (Cluster-6987.19844). All of the DkbHLH proteins with a lower GRAVY index (GRAVY < 0) were considered to be more water-soluble (Table 1).

**Table 1.** A list of all bHLH genes identified in the *D. kaki* from the transcriptome unigenes.

GeneID	pI	MW	aa	Instability Index	GRAVY	Description	Family Group
Cluster-15548.1	5.92	70,353.3	622	57.15	−0.493	bHLH-MYC and R2R3-MYB transcription factors N-terminal	III <sub>f</sub>
Cluster-16159.0	8.59	33,034.44	297	70.62	−0.511	Helix–loop–helix DNA-binding domain	V <sub>b</sub>
Cluster-17193.0	7.14	29,350.72	271	44.77	−0.648	Helix–loop–helix DNA-binding domain	XII
Cluster-17857.0	10.79	21,843.76	194	60.57	−0.242	Helix–loop–helix DNA-binding domain	VII <sub>b</sub>
Cluster-19711.0	9.26	27,915.6	247	42.38	−0.266	Helix–loop–helix DNA-binding domain	I <sub>b</sub>
Cluster-19936.1	5.94	52,936.87	472	53.04	−0.464	Helix–loop–helix DNA-binding domain	X
Cluster-20268.0	9.42	22,594.14	199	58.5	−0.573	Helix–loop–helix DNA-binding domain	I <sub>b</sub>
Cluster-3934.0	10.3	19,350.09	175	64.74	−0.582	Helix–loop–helix DNA-binding domain	VIII <sub>b</sub>
Cluster-6987.10497	5.7	63,669.96	574	54.13	−0.656	bHLH-MYC and R2R3-MYB transcription factors N-terminal	III <sub>e</sub>
Cluster-6987.10953	4.52	13,939.64	123	64.48	−0.468	Helix–loop–helix DNA-binding domain	III <sub>c</sub>
Cluster-6987.12368	8.32	39,649.34	357	55.24	−0.618	Helix–loop–helix DNA-binding domain	I <sub>b</sub>
Cluster-6987.12953	5.85	57,668.09	535	75.43	−0.549	Helix–loop–helix DNA-binding domain	VII <sub>a</sub>

Table 1. Cont.

GeneID	pI	MW	aa	Instability Index	GRAVY	Description	Family Group
Cluster-6987.13574	6.54	30,618.32	276	47.1	−0.551	Helix–loop–helix DNA-binding domain	Vb
Cluster-6987.15443	5.9	27,730.39	250	56.36	−0.534	Helix–loop–helix DNA-binding domain	IVc
Cluster-6987.16197	5.42	54,988.88	499	52.74	−0.378	bHLH-MYC and R2R3-MYB transcription factors N-terminal	IIIe
Cluster-6987.1658	9.56	30,647.86	277	62.46	−0.626	Helix–loop–helix DNA-binding domain	IVa
Cluster-6987.17178	5.4	37,385.92	335	62.07	−0.523	Helix–loop–helix DNA-binding domain	Ia
Cluster-6987.18061	4.62	37,271.96	334	53.27	−0.478	Helix–loop–helix DNA-binding domain	IIIb
Cluster-6987.19137	4.97	42,060.74	373	52.02	−0.515	Helix–loop–helix DNA-binding domain	IIIb
Cluster-6987.19492	8.2	47,950.04	433	50.54	−0.527	bHLH-MYC and R2R3-MYB transcription factors N-terminal	IIIId
Cluster-6987.19614	6.29	28,597.66	253	62.5	−0.385	Helix–loop–helix DNA-binding domain	IIIc
Cluster-6987.19844	5.22	39,283.15	352	65.05	−0.841	Helix–loop–helix DNA-binding domain	Va
Cluster-6987.20382	9.79	12,432.12	108	82.07	−0.719	Helix–loop–helix DNA-binding domain	XII
Cluster-6987.21517	6.4	44,681.21	406	54.06	−0.488	bHLH-MYC and R2R3-MYB transcription factors N-terminal	IIIId
Cluster-6987.2220	8.23	37,059.51	329	63.87	−0.243	Helix–loop–helix DNA-binding domain	VIIIb
Cluster-6987.22341	9.17	47,990.27	433	44.05	−0.563	bHLH-MYC and R2R3-MYB transcription factors N-terminal	IIIId
Cluster-6987.22813	6.73	26,070.62	238	52.85	−0.642	Helix–loop–helix DNA-binding domain	IVc
Cluster-6987.23320	9.32	28,111.55	252	59.86	−0.379	Helix–loop–helix DNA-binding domain	VIIIb
Cluster-6987.24255	5.97	23,415.91	211	55.17	−0.237	Helix–loop–helix DNA-binding domain	XI
Cluster-6987.25515	5.39	62,110.75	574	50.52	−0.48	Helix–loop–helix DNA-binding domain	XII
Cluster-6987.28059	6.69	32,511.04	297	49.9	−0.725	Helix–loop–helix DNA-binding domain	Va
Cluster-6987.28409	6.37	50,973.69	474	52.91	−0.489	Helix–loop–helix DNA-binding domain	VIIb
Cluster-6987.28853	6.35	79,061.33	720	50.46	−0.568	bHLH-MYC and R2R3-MYB transcription factors N-terminal	IIIe
Cluster-6987.29876	9.95	30,252.81	282	34.57	−0.016	Helix–loop–helix DNA-binding domain	XI
Cluster-6987.3156	6.15	39,930.5	362	54.46	−0.3	Helix–loop–helix DNA-binding domain	IVa
Cluster-6987.31584	9.57	19,032.99	166	48.38	−0.74	Helix–loop–helix DNA-binding domain	IVc
Cluster-6987.334	5.87	44,580.72	397	51.11	−0.452	Helix–loop–helix DNA-binding domain	IVa
Cluster-6987.3486	5.49	35,928.41	323	64.54	−0.522	Helix–loop–helix DNA-binding domain	Ia
Cluster-6987.36402	6.3	40,786.68	372	49.98	−0.615	Helix–loop–helix DNA-binding domain	XII
Cluster-6987.38862	6.3	40,736.53	368	56.85	−0.835	Helix–loop–helix DNA-binding domain	IVb
Cluster-6987.40617	5.62	21,615.02	192	93.67	−0.755	Helix–loop–helix DNA-binding domain	VIIb
Cluster-6987.40946	9.61	45,283.41	422	52.67	−0.574	Helix–loop–helix DNA-binding domain	IX
Cluster-6987.43498	6.29	23,122.8	216	48.76	−0.123	Helix–loop–helix DNA-binding domain	VIIIb
Cluster-6987.43499	9.44	8641.81	76	77.43	−0.779	Helix–loop–helix DNA-binding domain	VIIa
Cluster-6987.43501	6.01	62,262.63	584	46.58	−0.517	Helix–loop–helix DNA-binding domain	VIIa
Cluster-6987.44311	6.1	36,970.1	335	37.89	−0.31	Helix–loop–helix DNA-binding domain	IVa
Cluster-6987.52370	8.67	61,252.56	564	58.26	−0.61	Helix–loop–helix DNA-binding domain	XII
Cluster-6987.52499	5.91	39,534.24	363	49.32	−0.596	Helix–loop–helix DNA-binding domain	XII
Cluster-6987.53117	9.11	35,833.89	319	55.41	−0.522	Helix–loop–helix DNA-binding domain	VIIa
Cluster-6987.53178	8.65	51,919.33	468	51.1	−0.707	Helix–loop–helix DNA-binding domain	IX
Cluster-6987.54023	7.2	40,160.13	356	52.22	−0.714	Helix–loop–helix DNA-binding domain	XII
Cluster-6987.5405	6.5	43,291.31	395	56.64	−0.564	Helix–loop–helix DNA-binding domain	VIIb
Cluster-6987.5906	5.84	38,000.7	345	59.52	−0.532	Helix–loop–helix DNA-binding domain	VIIIb
Cluster-6987.6381	5.76	28,349.49	262	65.3	−0.589	Helix–loop–helix DNA-binding domain	IX
Cluster-6987.6880	8.4	26,783.4	246	44.78	−0.373	Helix–loop–helix DNA-binding domain	Vb
Cluster-6987.7477	6.06	27,388.11	241	57.5	−0.591	Helix–loop–helix DNA-binding domain	VIIIb
Cluster-6987.8842	6.52	27,533.95	251	55.93	−0.668	Helix–loop–helix DNA-binding domain	XII
Cluster-6987.899	9.19	25,377.21	231	66.65	−0.442	Helix–loop–helix DNA-binding domain	VIIIb
Cluster-76.0	9.5	12,131.7	105	70.54	−0.77	Helix–loop–helix DNA-binding domain	XII

Note: if instability index is greater than 40, it is an unstable protein; if instability index is less than 40, it belongs to a stable protein; grand aversion of hydrophilicity (GRAVY); larger negative values indicate better hydrophilicity and larger positive values indicate greater hydrophobia.

### 3.2. Phylogenetic Analysis of the bHLH Proteins

To investigate the evolutionary relationships of the bHLH proteins, the NJ phylogenetic tree was constructed between *D. kaki* and *A. thaliana* (Figure 1). The DkbHLH proteins were classified under the previous classification of AtbHLH [28]. The DkbHLH proteins were divided into 12 groups, from I to XII. Group III contained 12, the largest number of DkbHLH proteins, while groups II, VI, and X did not have any DkbHLH proteins. Combining the phylogenetic analysis with conserved domain analysis, DkbHLH proteins

in groups III (d, e, and f) contained the bHLH-MYC and R2R3-MYB transcription factor N-terminal domains.

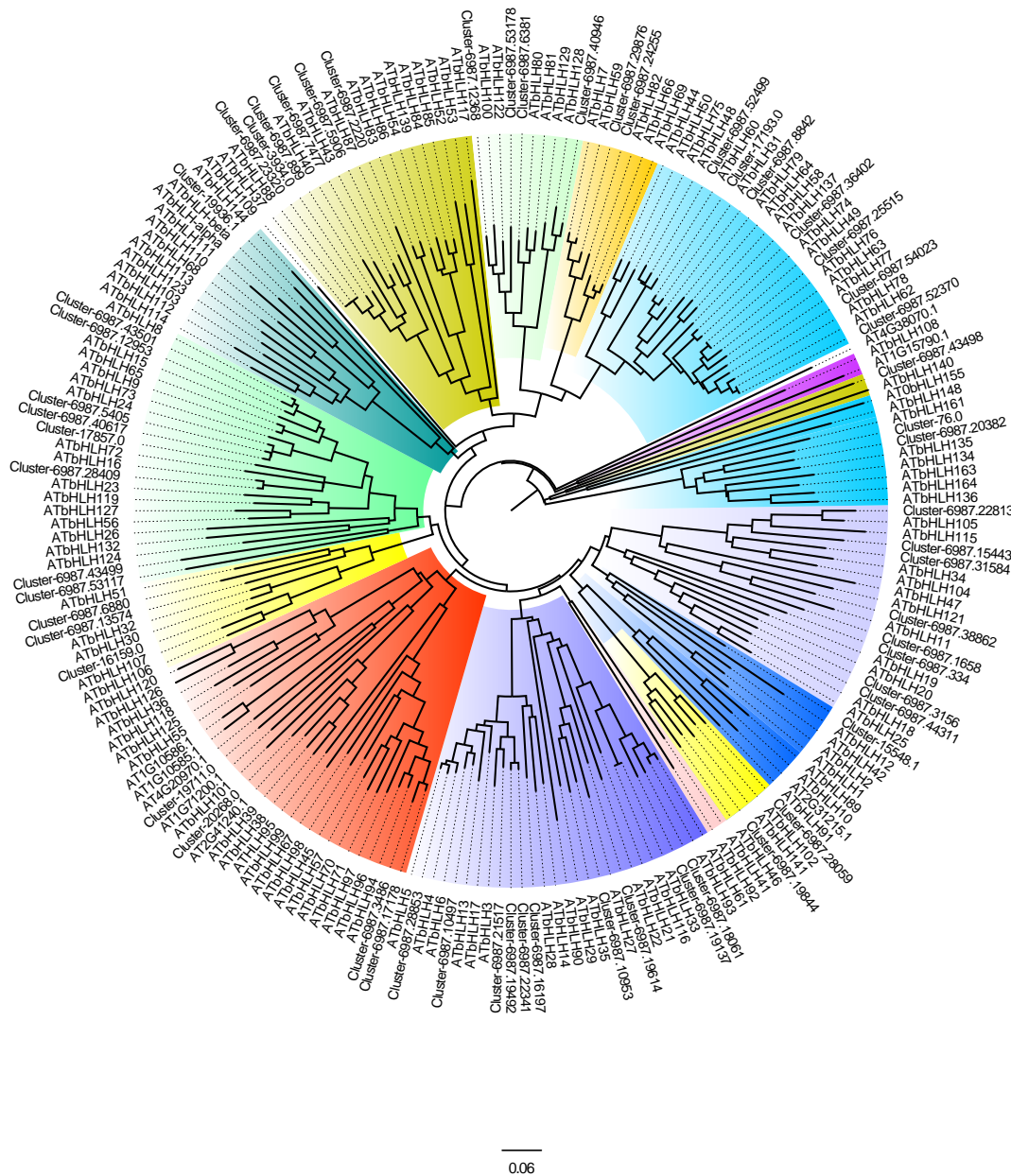


**Figure 1.** Phylogenetic analysis of the *D. kaki* bHLH proteins compared to *A. thaliana*. Different colours represent different family groups, and the detail groups are shown in Table 1.

### 3.3. Conserved Motif Analysis

The predicted DkbHLH amino acid sequence conserved motif characteristics were analysed using the MEME tool (Figure 2). A total of nine motifs were predicted in the 59 bHLH members and labelled as Motifs 1–9. The lengths of the motifs ranged from 9 to 35 amino acids. Motifs 1 and 2 were present in nearly all DkbHLH proteins. Proteins in Groups VII and IX only contained these two motifs. Furthermore, Motifs 6 and 7 were identified in Groups I, III (d and e), and V; Motifs 8 and 9 were only present in Group XII; Motif 4 was identified in Group VIII; and Motif 5 was only observed in Group III (f). Most of the DkbHLH proteins in the same group possessed the same conserved motifs as in the phylogenetic analysis.

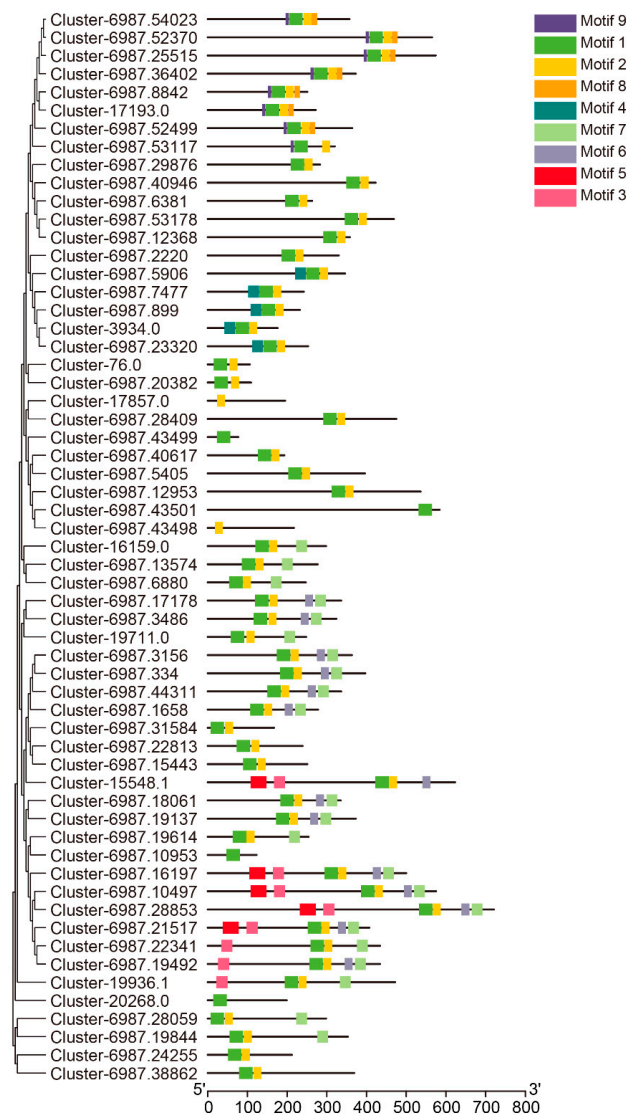


**Figure 2.** Phylogenetic tree (left) and the conserved motifs (right) of the *D. kaki* bHLH proteins. Different colours represent different motifs.

### 3.4. Gene Ontology Annotation

The functional associations were identified using GO term enrichment analysis among the *DkbHLH* proteins with agriGO (Figure 3). Sixty annotations were assigned to GO terms and summarised in three primary functional categories, including the cellular component, molecular function, and biological process. Three groups, including binding (GO:0005488), protein binding (GO:0005515), and protein dimerisation activity (GO:0046983) were the significant classifications for all of the *DkbHLH* genes.

### 3.5. Selection Pressure and Differentiation Time of the Homologous bHLH Genes

To further analyse the selection pressure and differentiation time of paralogous *DkbHLH* gene pairs and orthologous *bHLH* gene pairs between *D. kaki* and *A. thaliana*, the  $K_a:K_s$  ratio was calculated (Table 2). Surprisingly, the  $K_a:K_s$  ratio of all paralogous and orthologous gene pairs was less than one, demonstrating that these *bHLH* genes are under purifying selection. The differentiation time of paralogous *bHLH* gene pairs in *D. kaki* was between 77 and 136 MYA, and the differentiation time of orthologous *bHLH* genes between *D. kaki* and *A. thaliana* was between 137 and 266 MYA.

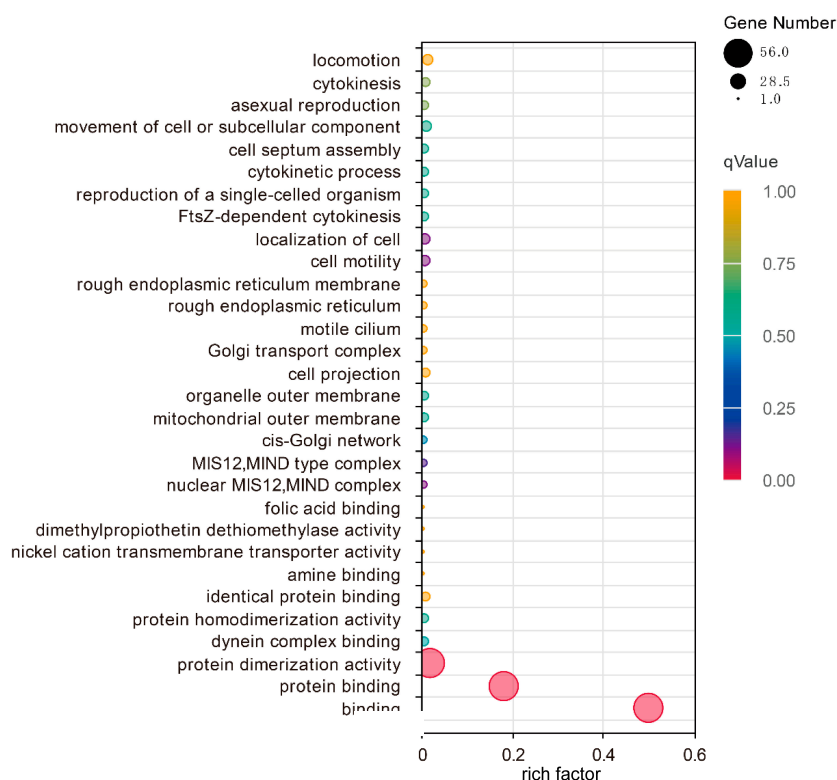


**Figure 3.** GO annotation of 59 *bHLH* transcription factors. The dot size represents gene number, and different colours represent the values of the qValue.

**Table 2.** Ka, Ks, and Ka:Ks values between homologous *bHLH* gene pairs.

Seq_1	Seq_2	Ka	Ks	Ka:Ks	Differentiation Time
Cluster-6987.17178	Cluster-6987.3486	0.34702	1.659578	0.209101	136.031
Cluster-6987.38862	AtbHLH011	0.532813	3.251332	0.163875	266.5026
Cluster-6987.5405	AtbHLH024	0.605611	2.374446	0.255054	194.6267
Cluster-6987.28409	AtbHLH016	0.223524	2.046914	0.1092	167.7798
Cluster-6987.25515	AtbHLH049	0.372177	1.674926	0.222205	137.289
Cluster-6987.36402	AtbHLH074	0.444855	2.575702	0.172712	211.1231
Cluster-6987.22813	AtbHLH105	0.165583	2.098734	0.078897	172.0274
Cluster-6987.22341	Cluster-6987.19492	0.17841	0.939712	0.189856	77.02557
Cluster-6987.21517	AtbHLH003	0.344623	1.905672	0.18084	156.2026
Cluster-6987.5906	AtbHLH087	0.449166	2.025877	0.221714	166.0555

### 3.6. *bHLH* and *MYB* Protein–Protein Interaction Network Analysis

The protein–protein interactions between *DkbHLH* and *DkMYB* proteins were analysed using the STRING database (Figure 4). The *D. kaki* protein sequence of *bHLH*\_Cluster-15548.1 showed similarity to the *AtGL3* (AT5G41315.1) protein with a 538.5-bit score and 48.7 identities. *bHLH*\_Cluster-15548.1 interacted with other *bHLH* and *MYB* proteins with combined scores from 0.411 to 0.99. The predicted functional partners of Cluster-15548.1, including *MYB*\_Cluster-6987.24679, *MYB*\_Cluster-6987.15450, *MYB*\_Cluster-6987.38210, *bHLH*\_Cluster-6987.21517, *MYB*\_Cluster-6987.43699, *MYB*\_Cluster-6987.3798, *MYB*\_Cluster-6987.38499, and *MYB*\_Cluster-6987.4705, were associated with a flavonoid biosynthetic process and RNA polymerase II transcription regulator recruiting activity. *bHLH*\_Cluster-6987.21517 is an *AtbHLH3* (AT4G16430) homolog with a 339-bit score and 46.1 identities and could interact with other *bHLH* and *MYB* proteins with combined scores from 0.525 to 0.567. The predicted functional partners of *bHLH*\_Cluster-6987.21517, including *MYB*\_Cluster-6987.24679, *MYB*\_Cluster-6987.15450, *bHLH*\_Cluster-6987.21517, and

MYB\_Cluster-6987.38499, were associated with flavonoid and proanthocyanidin biosynthetic processes.

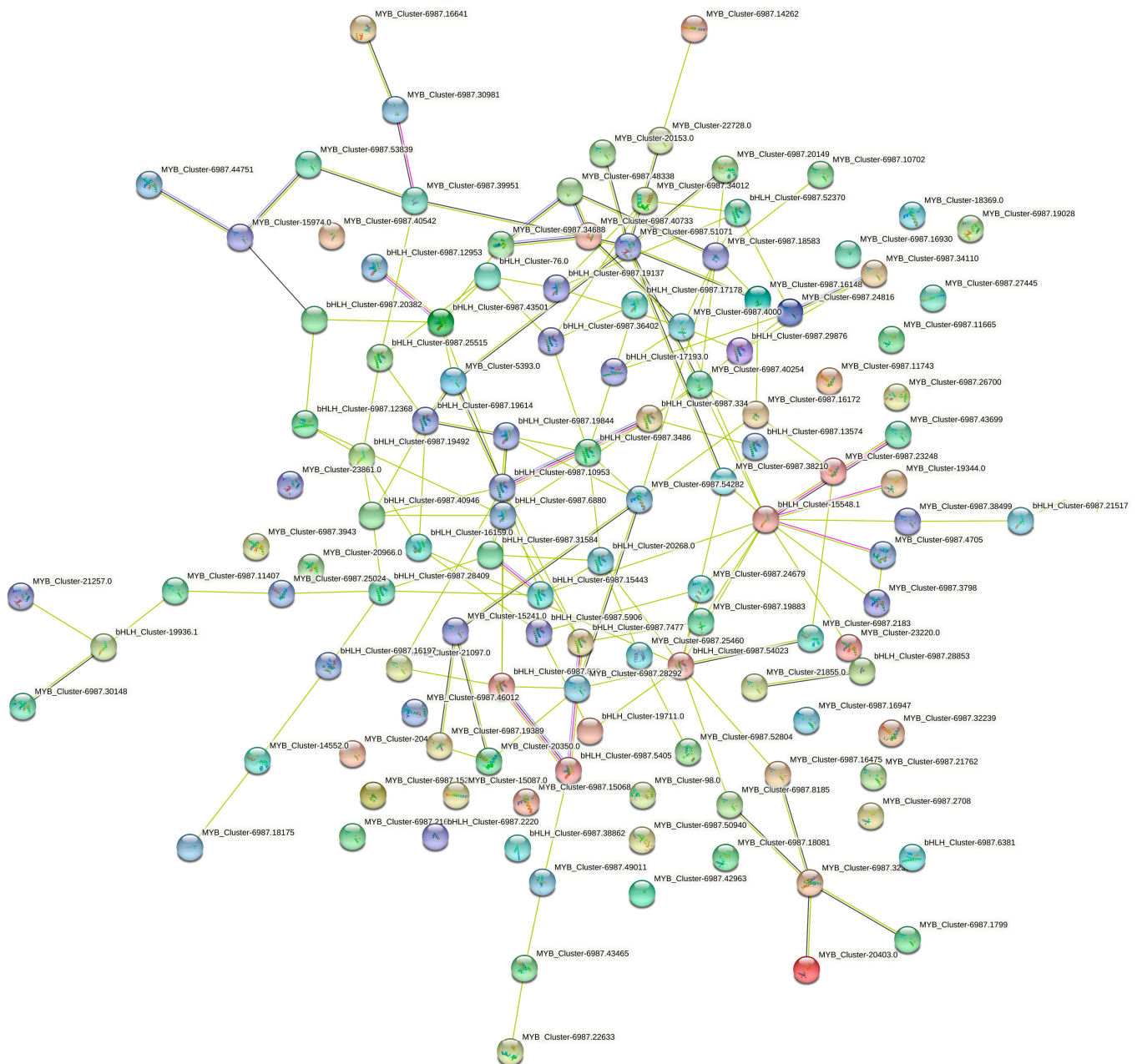
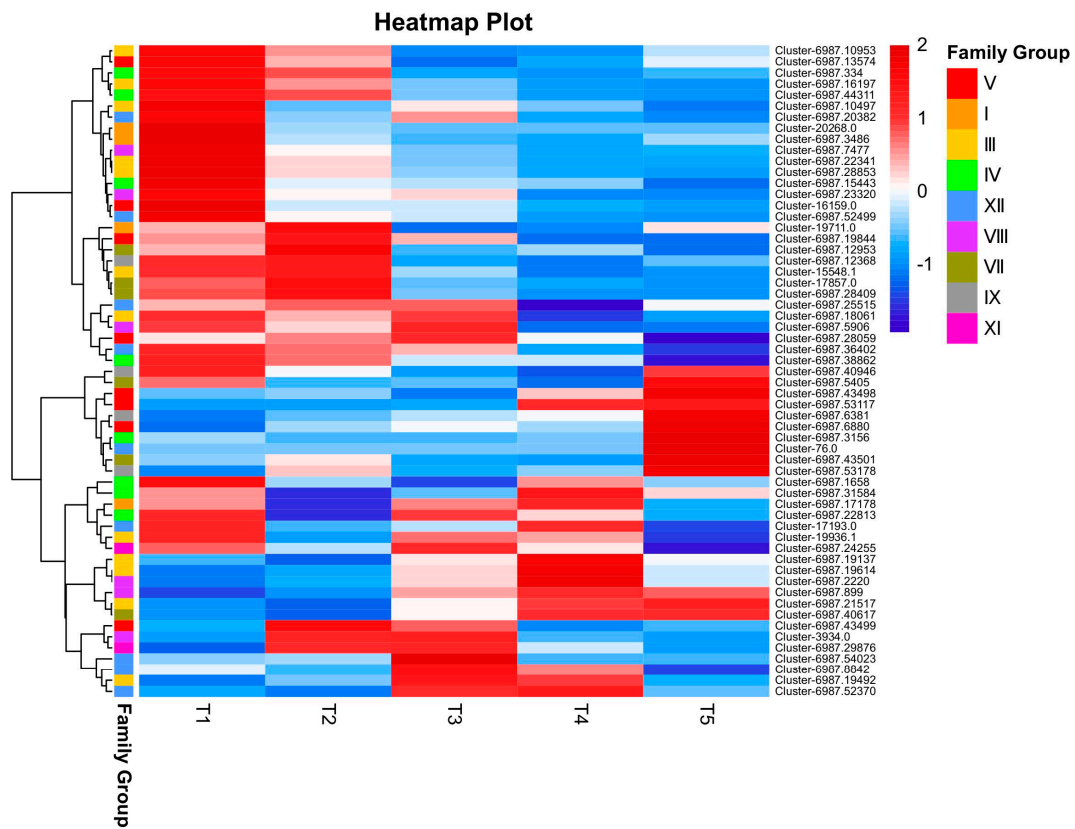


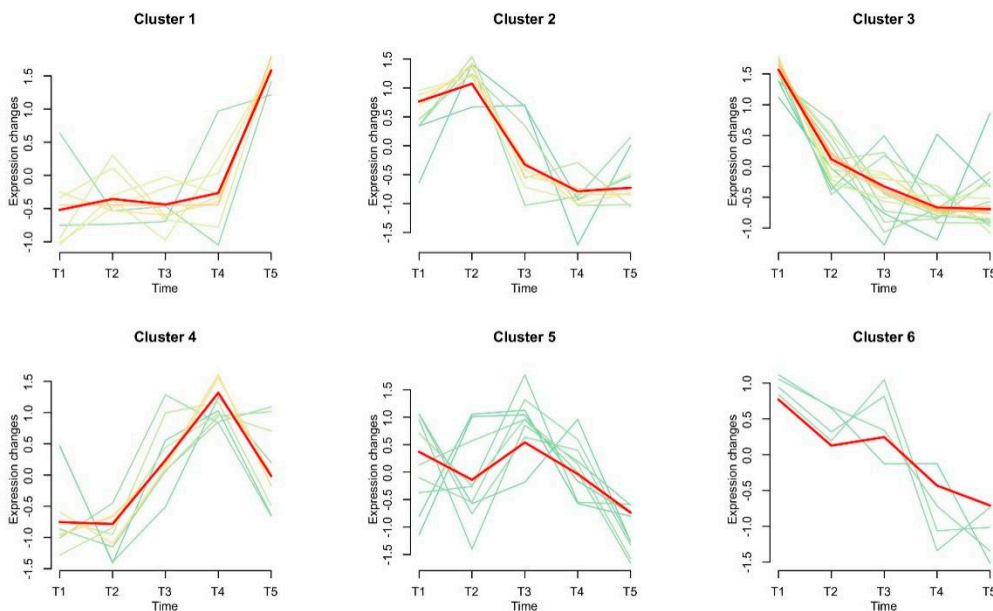
**Figure 4.** The protein–protein interaction network between bHLH and MYB proteins. Different colours have no additional meaning.

### 3.7. *In Silico* Analysis of *bHLH* Genes in *D. kaki* Fruit at Five Different Stages

The expression patterns of *DkbHLH* genes in the fruit at five different developmental stages were analysed using RNA-seq. Distinct *bHLH* gene clusters exhibited time-specific expression profiles in persimmon fruit development (Figure 5a,b). Genes in Cluster 3 were highly expressed in T1 and showed a downregulated trend; genes in Cluster 2 reached the highest expression in T2; genes in Cluster 1, whose expression peaked at T5, were differentially upregulated between T4 and T5; genes in Clusters 4, 5, and 6 peaked at T4, T3, and T1, respectively.



(a)



(b)

**Figure 5.** Gene expression analysis of bHLH genes in *D. kaki* fruit at five stages. (a) Heat map clustering of *DkbHLH* gene expression levels at five developmental stages; heatmaps depict the normalised gene expression values, which represent the mean value of three biological replicates. (b) Clustering analysis of *DkbHLH* genes.

#### 4. Discussion

Persimmon is an important fruit crop in east Asia. The high PA content leads to fruit astringency, the critical characteristic of persimmon. The natural de-astringency of C-PCNA persimmon is associated with both the “coagulation effect” and “dilution effect”. Previous studies have shown that bHLH and MYB may associate with PA biosynthesis in *Lotus* species [35], *Freesia hybrida* [36], and *Anthurium andraeanum* [37]. However, only a few MYB and bHLH genes, such as DkMYB4 and DkMYB14, are the key transcription factors for the natural astringency of Japanese PCNA (J-PCNA) and C-PCNA persimmon, respectively [38,39]. Su et al. [40] isolated a novel *bHLH* gene DkMYC1 from persimmon that may be associated with PA biosynthesis via the regulation of structural genes such as *DkDHD*, *DkF3'5'H*, and *DkANR*. In addition, DkbHLH1 was strongly induced by an artificially high CO<sub>2</sub> atmosphere in three astringent-type persimmons [41]. The mechanisms of the *bHLH* TFs' involvement in PA biosynthesis are currently unknown. In this study, 59 *bHLH* TFs were identified, and their phylogenetic relationships with *A. thaliana* were analysed. The expression patterns of five developmental stages of the C-PCNA persimmon were analysed, providing a theoretical basis for further study of the natural de-astringency of PCNA persimmon.

Phylogenetic, motif, and conserved domain analyses of proteins were used to infer biological functions. Phylogenetic analysis demonstrated that five DkbHLH proteins were clustered into groups III (d, e, and f) containing *bHLH-MYC* and *R2R3-MYB* TF N-terminal domains. bHLH members of III (f) play essential roles in anthocyanin synthesis [9,10]. Genes clustered in the same group commonly exhibited similar structures and functions. The *AtbHLH001* (*GL3*), *AtbHLH002* (*EGL3*), and *AtbHLH042* (*TT8*) genes are the critical regulators of anthocyanin and PA biosynthesis [41–43]. Only one bHLH member (Cluster-15548.1) clustered into Group III (f) contained the *bHLH-MYC* and *R2R3-MYB* TF N-terminal domains, possibly involved in PA biosynthesis. Motif 5 was only detected in group III (f) and may be associated with its specific function in PA biosynthesis.

Furthermore, the protein–protein interaction analysis between DkbHLH and DkMYB demonstrated that the *D. kaki* bHLH\_Cluster-15548.1 protein sequence exhibited high similarity to the AtGL3 (AT5G41315.1) protein, which is associated with flavonoid and PA biosynthesis. Previous studies have shown that 120 (T3) to 140 (T4) DAF may be the critical phase for the “dilution effect”, and 140 (T4) to 160 (T5) DAF may be the crucial phase for the “coagulation effect” [20]. Therefore, the expression patterns of the bHLH gene family members were analysed in the *D. kaki* ‘Xiaoguotianshi’ cultivar at five developmental stages. Surprisingly, Cluster-15548.1 was differentially downregulated at T4 compared to T3, which may be associated with the “dilution effect”. However, the function of Cluster-15548.1 still requires further investigation.

#### 5. Conclusions

A total of 59 *bHLH* family members have been identified from the “Xiaoguotianshi” persimmon transcriptome data. These proteins were clustered into 12 groups from I to XII based on their phylogenetic relationships with *Arabidopsis thaliana*. Combined with the phylogenetic analysis, in silico expression patterns of five developmental stages, and the protein–protein interaction analysis between DkbHLH and DkMYB proteins, the bHLH\_Cluster-15548.1 protein sequence was identified to be highly similar to the AtGL3 (AT5G41315.1) protein, which is associated with flavonoid and PA biosynthesis. This study presented the systematic analysis of *bHLH* genes from *D. kaki* and provided valuable information for further research on the involvement of bHLH protein in PA and anthocyanin biosynthesis.

**Author Contributions:** L.H. and J.F. designed the experiments. Q.Z., Y.S., H.L., S.D. and P.S. offered meaningful feedback and assisted form the research. W.H. conducted the analysis and wrote the manuscript. All authors have read and agreed to the published version of the manuscript.

**Funding:** This work was financially supported by the National Natural Science Foundation of China (32071801) and the National Key R&D Program of China (2019YFD1000600).

**Institutional Review Board Statement:** Not applicable.

**Informed Consent Statement:** Not applicable.

**Data Availability Statement:** Not applicable.

**Conflicts of Interest:** The authors declare no conflict of interest.

## References

1. Castillon, A.; Shen, H.; Huq, E. Phytochrome interacting factors: Central players in phytochrome-mediated light signaling networks. *Trends Plant Sci.* **2007**, *12*, 514–521. [[CrossRef](#)]
2. Duek, P.D.; Fankhauser, C. HFR1, a putative *bHLH* transcription factor, mediates both phytochrome a and cryptochrome signaling. *Plant J.* **2003**, *34*, 827–836. [[CrossRef](#)] [[PubMed](#)]
3. Kondou, Y.; Nakazawa, M.; Kawashima, M.; Ichikawa, T.; Yoshizumi, T.; Suzuki, K.; Ishikawa, A.; Koshi, T.; Matsui, R.; Muto, S. RETARDED GROWTH OF EMBRYO1, a new basic helix-loop helix protein, in endosperm to control EMBRYO growth. *Plant Physiol.* **2008**, *147*, 1924–1935. [[CrossRef](#)]
4. Toledo-Ortiz, G.; Huq, E.; Quail, P.H. The Arabidopsis basic/helix-loop-helix transcription factor family. *Plant Cell* **2003**, *15*, 1749–1770. [[CrossRef](#)] [[PubMed](#)]
5. Wang, R.; Peng, Z.; Kong, N.; Lu, R.; Pei, Y.; Huang, C.; Ma, H. Genome-wide identification and characterization of the Potato *bHLH* transcription factor family. *Genes* **2018**, *9*, 54. [[CrossRef](#)] [[PubMed](#)]
6. Sun, H.; Fan, H.J.; Ling, H.Q. Genome-wide identification and characterization of the *bHLH* gene family in tomato. *BMC Genom.* **2015**, *16*, 9. [[CrossRef](#)]
7. Mao, K.; Dong, Q.; Li, C.; Liu, C.; Ma, F. Genome wide identification and characterization of apple *bHLH* transcription factors and expression analysis in response to drought and salt stress. *Front. Plant Sci.* **2017**, *8*, 480. [[CrossRef](#)]
8. Li, X.; Duan, X.; Jiang, H.; Sun, Y.; Tang, Y.; Yuan, Z.; Guo, J.; Liang, W.; Chen, L.; Yin, J.; et al. Genome-wide analysis of basic/helix-loop-helix transcription factor family in rice and *Arabidopsis*. *Plant Physiol.* **2006**, *141*, 1167–1184. [[CrossRef](#)]
9. Song, S.; Qi, T.; Fan, M.; Zhang, X.; Gao, H.; Huang, H.; Wu, D.; Guo, H.; Xie, D. The *bHLH* subgroup IIIId factors negatively regulate jasmonate-mediated plant defense and development. *PLoS Genet.* **2013**, *9*, e1003653. [[CrossRef](#)]
10. Liu, X.; An, X.; Liu, X.; Hu, D.; Wang, X.; You, C.; Hao, Y. *MdSnRK1.1* interacts with *MdJAZ18* to regulate sucrose-induced anthocyanin and proanthocyanidin accumulation in apple. *J. Exp. Bot.* **2017**, *68*, 2977–2990. [[CrossRef](#)]
11. Chandler, V.L.; Radicella, J.P.; Robbins, T.P.; Chen, J.; Turks, D. Two regulatory genes of the maize anthocyanin pathway are homologous: Isolation of B utilizing R genomic sequences. *Plant Cell* **1989**, *1*, 1175–1183. [[PubMed](#)]
12. Payne, C.T.; Zhang, F.; Lloyd, A.M. GL3 encodes a *bHLH* protein that regulates trichome development in *Arabidopsis* through interaction with GL1 and TTG1. *Genetics* **2000**, *156*, 1349–1362. [[CrossRef](#)]
13. Li, M.; Sun, L.; Gu, H.; Cheng, D.; Guo, X.; Chen, R.C.; Wu, Z.; Jiang, J.; Fan, X.; Chen, J. Genome-wide characterization and analysis of *bHLH* transcription factors related to anthocyanin biosynthesis in spine grapes (*Vitis davidii*). *Sci. Rep.* **2021**, *11*, 6863. [[CrossRef](#)]
14. Zhang, F.; Gonzalez, A.; Zhao, M.; Payne, C.T.; Lloyd, A. A network of redundant *bHLH* proteins functions in all TTG1-dependent pathways of *Arabidopsis*. *Development* **2003**, *130*, 4859–4869. [[CrossRef](#)] [[PubMed](#)]
15. Neuffer, M.G.; Coe, E.H.; Wessler, S.R. *Mutants of Maize*, 1st ed.; Cold Spring Harbor Laboratory Press: New York, NY, USA, 1997; pp. 54–59.
16. Petroni, K.; Cominelli, E.; Consonni, G.; Gusmaroli, G.; Gavazzi, G.; Tonelli, C. The developmental expression of the maize regulatory gene Hopi determines germination-dependent anthocyanin accumulation. *Genetics* **2000**, *155*, 323–336. [[CrossRef](#)] [[PubMed](#)]
17. Rahim, M.A.; Busatto, N.; Trainotti, L. Regulation of anthocyanin biosynthesis in peach fruits. *Planta* **2014**, *240*, 913–929. [[CrossRef](#)]
18. Hichri, I.; Heppel, S.C.; Pillet, J.; Leon, C.; Czemm, S.; Delrot, S.; Virginie, L.; Bogs, J. The basic helix-loop-helix transcription factor *MYC1* is involved in the regulation of the flavonoid biosynthesis pathway in grapevine. *Mol. Plant* **2010**, *3*, 509–523. [[CrossRef](#)]
19. Wada, T.; Kunihiro, A.; Tominaga-Wada, R.; Takaya, M. *Arabidopsis* CAPRICE (MYB) and GLABRA3 (*bHLH*) control tomato (*Solanum lycopersicum*) anthocyanin biosynthesis. *PLoS ONE* **2014**, *9*, e109093. [[CrossRef](#)]
20. Wang, Y.; Zhang, Q.; Pu, T.; Suo, Y.; Han, W.; Diao, S.; Li, H.; Sun, P.; Fu, J. Transcriptomic profiling analysis to identify genes associated with PA biosynthesis and insolubilization in the late stage of fruit development in C-PCNA persimmon. *Sci. Rep.* **2022**, *12*, 19140. [[CrossRef](#)]
21. Punta, M.; Coghill, P.C.; Eberhardt, R.Y.; Mistry, J.; Tate, J.; Boursnell, C.; Pang, N.; Forslund, K.; Ceric, G.; Clements, J. The Pfam protein families database. *Nucleic Acids Res.* **2004**, *28*, 263–266. [[CrossRef](#)]
22. Wilkins, M.R.; Gasteiger, E.; Bairoch, A.; Sanchez, J.C.; Williams, K.L.; Appel, R.D.; Hochstrasser, D.F. Protein identification and analysis tools in the Expasy server. *Methods Mol. Biol.* **1999**, *112*, 531–552. [[PubMed](#)]

23. Jin, J.P.; Tian, F.; Yang, D.C.; Meng, Y.Q.; Kong, L.; Luo, J.C.; Gao, G. PlantTFDB 4.0: Toward a central hub for transcription factors and regulatory interactions in plants. *Nucleic Acids Res.* **2017**, *45*, D1040–D1045. [[CrossRef](#)] [[PubMed](#)]
24. Jin, J.P.; He, K.; Tang, X.; Li, Z.; Lv, L.; Zhao, Y.; Luo, J.C.; Gao, G. An *Arabidopsis* transcriptional regulatory map reveals distinct functional and evolutionary features of novel transcription factors. *Mol. Biol. Evol.* **2015**, *32*, 1767–1773. [[CrossRef](#)] [[PubMed](#)]
25. Jin, J.P.; Zhang, H.; Kong, L.; Gao, G.; Luo, J.C. PlantTFDB 3.0: A portal for the functional and evolutionary study of plant transcription factors. *Nucleic Acids Res.* **2014**, *42*, D1182–D1187. [[CrossRef](#)]
26. Larkin, M.A.; Blackshields, G.; Brown, N.P.; Chenna, R.; Mcgettigan, P.A.; McWilliam, H.; Valentin, F.; Wallace, I.M.; Wilm, A.; Lopez, R. Clustal W and Clustal X version 2.0. *Bioinformatics* **2007**, *21*, 2947–2948. [[CrossRef](#)]
27. Tamura, K.; Peterson, D.; Peterson, N.; Stecher, G.; Nei, M.; Kumar, S. MEGA5: Molecular evolutionary genetics analysis using maximum likelihood, evolutionary distance, and maximum parsimony methods. *Mol. Biol. Evol.* **2011**, *28*, 2731–2739. [[CrossRef](#)]
28. Heim, M.A.; Jakoby, M.; Werber, M.; Martin, C.; Weisshaar, B.; Bailey, P.C. The basic helix-loop-helix transcription factor family in plants: A genome-wide study of protein structure and functional diversity. *Mol. Biol. Evol.* **2003**, *20*, 735–747. [[CrossRef](#)]
29. Bailey, T.L.; Johnson, J.; Grant, C.E.; Noble, W.S. The MEME suite. *Nucleic Acids Res.* **2015**, *43*, W39–W49. [[CrossRef](#)]
30. Szklarczyk, D.; Gable, A.L.; Lyon, D.; Junge, A.; Wyder, S.; Huerta-Cepas, J.; Simonovic, M.; Doncheva, N.T.; Morris, J.H.; Bork, P. STRING v11: Protein-protein association networks with increased coverage, supporting functional discovery in genome-wide experimental datasets. *Nucleic Acids Res.* **2018**, *47*, D607–D613. [[CrossRef](#)]
31. Li, W.H.; Gojobori, T.; Nei, M. Pseudogenes as a paradigm of neutral evolution. *Nature* **1981**, *292*, 237–239. [[CrossRef](#)]
32. Chen, C.; Chen, H.; Zhang, Y.; Thomas, H.R.; Xia, R. TBtools: An integrative toolkit developed for interactive analyses of big biological data. *Mol. Plant.* **2020**, *13*, 1194–1202. [[CrossRef](#)]
33. Wang, J.; Sun, P.; Li, Y.; Liu, Y.; Yu, J.; Ma, X.; Sun, S.; Yang, N.; Xia, R.; Lei, T. Hierarchically aligning 10 legume genomes establishes a family-level genomics platform. *Plant Physiol.* **2017**, *174*, 1981–2016. [[CrossRef](#)]
34. Li, J.F.; Miao, B.B.; Wang, S.X.; Dong, W.X.; Hou, S.; Si, C.C.; Wang, M.J. Hiplot: A comprehensive and easy-to-use web service for boosting publication-ready biomedical data visualization. *Brief Bioinform.* **2022**, *23*, bbac261. [[CrossRef](#)] [[PubMed](#)]
35. Escaray, F.J.; Passeri, V.; Perea-García, A.; Antonelli, C.J.; Damiani, F.; Ruiz, O.A.; Paolucci, F. The R2R3-MYB TT2b and the bHLH TT8 genes are the major regulators of proanthocyanidin biosynthesis in the leaves of Lotus species. *Planta* **2017**, *246*, 243–261. [[CrossRef](#)]
36. Li, Y.; Shan, X.; Zhou, L.; Gao, R.; Yang, S.; Wang, S.; Wang, L.; Gao, X. The R2R3-MYB factor *FhMYB5* from *Freesia hybrida* contributes to the regulation of anthocyanin and proanthocyanidin biosynthesis. *Front. Plant Sci.* **2019**, *9*, 1935. [[CrossRef](#)]
37. Li, C.; Qiu, J.; Huang, S.; Yin, J.; Yang, G. AaMYB3 interacts with AabHLH1 to regulate proanthocyanidin accumulation in *Anthurium andraeanum* (Hort.)—Another strategy to modulate pigmentation. *Hortic. Res.* **2019**, *6*, 14. [[CrossRef](#)]
38. Akagi, T.; Ikegami, A.; Tsujimoto, T.; Kobayashi, S.; Sato, A.; Kono, A.; Yonemori, K. *DkMyb4* is a myb transcription factor involved in proanthocyanidin biosynthesis in persimmon fruit. *Plant Physiol.* **2009**, *151*, 2028–2045. [[CrossRef](#)]
39. Chen, W.; Xiong, Y.; Xu, L.; Zhang, Q.; Luo, Z. An integrated analysis based on transcriptome and proteome reveals deastringency-related genes in CPCNA persimmon. *Sci. Rep.* **2017**, *7*, 44671. [[CrossRef](#)] [[PubMed](#)]
40. Su, F.; Jia, H.; Zhang, Q.; Luo, Z. Isolation and characterization of a basic Helix-Loop-Helix transcription factor gene potentially involved in proanthocyanidin biosynthesis regulation in persimmon (*Diospyros kaki* Thunb.). *Sci. Hortic.* **2012**, *136*, 115–121. [[CrossRef](#)]
41. Feyissa, D.N.; Lovdal, T.; Olsen, K.M.; Slimestad, R.; Lillo, C. The endogenous GL3, but not EGL3, gene is necessary for anthocyanin accumulation as induced by nitrogen depletion in *Arabidopsis* rosette stage leaves. *Planta* **2009**, *230*, 747–754. [[CrossRef](#)]
42. Xu, W.; Grain, D.; Le Gourrierec, J.; Harscoët, E.; Berger, A.; Jauvion, V.; Dubos, C. Regulation of flavonoid biosynthesis involves an unexpected complex transcriptional regulation of TT8 expression, in *Arabidopsis*. *New Phytol.* **2013**, *198*, 59–70. [[CrossRef](#)] [[PubMed](#)]
43. Baudry, A.; Heim, M.A.; Dubreucq, B.; Caboche, M.; Weisshaar, B.; Lepiniec, L. TT2, TT8, and TTG1 synergistically specify the expression of BANYULS and proanthocyanidin biosynthesis in *Arabidopsis thaliana*. *Plant J.* **2004**, *39*, 366–380. [[CrossRef](#)] [[PubMed](#)]

**Disclaimer/Publisher’s Note:** The statements, opinions and data contained in all publications are solely those of the individual author(s) and contributor(s) and not of MDPI and/or the editor(s). MDPI and/or the editor(s) disclaim responsibility for any injury to people or property resulting from any ideas, methods, instructions or products referred to in the content.